DOE/ER/13636--T;
DOE/ER/13636--T2
DE92 040159

PROGRESS REPORT

Fracture Characterization using the Stoneley Wave:

Fractures or permeable structures in reservoirs are of great importance in the exploration and production of hydrocarbons. Heterogeneous layers in the formation are also of major significance. A very good example of such heterogeneous and permeable structures is the sand-shale sequence found in sedimentary formations. Full waveform acoustic logging offers an effective tool for characterizing these structures. The current technique most commonly used for modeling borehole acoustic wave propagation with heterogeneous formation structures is the finite difference method (Bhashvanija, 1983; Stephen et al., 1985). This technique can handle heterogeneity quite easily. However, the implementation of the method to a permeable porous formation is still a topic of research. Although wavenumber integration technique can be used to calculate wave propagation in homogeneous porous formations (Rosenbaum, 1974; Schmitt et al., 1988), it is very difficult, if not impossible, to apply such a technique to treat problems involving porous layer structures. In this study, we will show that if only the low-frequency Stoneley wave is used, the interaction of acoustic waves with borehole permeable structures can be much simplified. The objective of this study is to develop a theoretical model that can be used to calculate borehole Stoneley wave propagation across heterogeneous and permeable structures. As a result, the properties of such structures can be characterized by means of Stoneley wave measurements.

The Stoneley (or tube) wave has been used as a means of formation evaluation and fracture detection. This wave mode dominates the low-frequency portion of the full waveform acoustic log due to its relatively slow velocity and large amplitude. Because this wave is an interface wave, it is sensitive to such formation properties as density, moduli, and most importantly, permeability or fluid transmissivity. It is expected that any change of these properties due to a formation heterogeneity will result in the change of Stoneley propagation characteristics, allowing the heterogeneity to be characterized using Stoneley wave measurements. Borehole fractures are an example of such heterogeneity. Paillet and White (1982) observed that attenuation of the Stoneley wave occurs in the vicinity of permeable fractures. Hornby et al. (1989) showed that permeable fractures also give rise to reflected Stoneley waves. Theoretical studies using finite difference (Stephen et al., 1985) and other techniques (Hornby et al., 1989; Tang, 1990) have been carried out to model the effects of a borehole fracture. In all these models, the analogy of a parallel planar fluid layer was commonly adopted to represent the fracture. Laboratory model experiments that comply with this analogy have yielded results that agree with the theoretical results (Tang and Cheng, 1989; Hornby et al., 1989). Although both attenuation and reflection of the Stoneley wave are predicted by the plane-fracture model, it takes a rather large fracture aperture (on the order of a centimeter) to attenuate the Stoneley wave significantly. However, fractures with such apertures are rarely found in the field (Hornby et al., 1989), but Stoneley wave attenuation (up to 50% or more) across in situ fractures is commonly observed (Paillet, 1980; Hardin et al., 1987). Until now, there has not been an effective model to account for the significant Stoneley wave attenuation observed in the field. Paillet et al. (1989) suggested that in situ fractures may consist of an array of flow passages or fracture layers, instead of a single fluid layer. In this study, we substantiate this hypothesis by modeling fractures as a permeable zone in the formation. Key parameters that are used to characterize the permeable zone are thickness of the zone, permeability, fracture porosity, and tortuosity. Since the last three parameters are typical parameters of a porous medium, we can use the Biot-Rosenbaum theory (Rosenbaum, 1974) to model the Stoneley wave characteristics in the permeable zone. Tang et al. (1991) have recently developed a simple model for Stoneley propagation in permeable formations. This model yields results consistent with the analysis of Biot-Rosenbaum theory in the presence of a hard formation, but the formulation and calculation are much simplified. The use of this simple theory in modeling the permeable zone allows the development of a fast and efficient algorithm to characterize the effects of the zone on Stoneley waves.

We have formulated a simple theory based on a complex transmission analog that can be used to calculate Stoneley wave propagation across a variety of heterogeneous structures. Applying the theory to the case of a fluid-filled fracture, we found that our theory is fully consistent with the existing theory and accounts for the effect of the vertical extent of an inclined fracture. Of primary importance are the cases of a permeable porous layer and a fracture zone. The theoretical results show that both the transmission and reflection of Stoneley waves are sensitive to the fluid transport properties of the zone. When the zone is highly permeable, Stoneley waves transmitted across the zone can be largely attenuated or even eliminated. This result is particularly significant in explaining the strong Stoneley wave attenuation observed at major fracture zones, whereas it is very difficult to explain this strong attenuation in terms of the plane-fracture theory. An important application of the fracture zone theory is to use it to model the observed Stoneley wave transmission and reflection at fracture zones. By matching the amplitudes of the transmitted and reflected waves, the overall fluid transmissivity of the zone can be assessed. Furthermore, because of the simplicity and efficiency in calculating the forward model, an inversion procedure may be formulated based on the model, so that such parameters as permeability, porosity, and tortuosity of the zone can be estimated from the measured Stoneley wave data. The details are contained in Tang and Cheng (1992) and included here as Appendix A.

Joint Interpretation of Seismic Anisotropy using Full Waveform and Shear Wave Logs:

Borehole acoustic logging can provide information about the in-situ physical properties of subsurface formation. The common approach is to estimate formation P-wave velocity by picking the first arrival from conventional log data. Since the advance of full waveform logs, we can determine the S-wave velocity in "hard" or "fast" formations, where the formation shear wave velocity is higher than the compressional wave velocity in the borehole fluid, by measuring the moveout of the shear/pseudo-Rayleigh wave packet. In "soft" or "slow" formations this is not possible because there is no refracted shear/ pseudo-Rayleigh arrival. One can estimate the shear wave velocity by inverting the Stoneley wave velocity (Cheng and Toksöz, 1983; Stevens and Day, 1986). However, this only really works in an isotropic elastic formation. More recently the advance of direct shear wave logging using the flexural mode of the borehole makes the direct measurement of shear wave velocity in "soft" formations possible (Zemanek et al., 1984). There is additional information contained in the Stoneley waves such as the permeability of the formation (Rosenbaum, 1974; Schmitt et al., 1988). Furthermore, anisotropy affects the different wavemodes differently. The shear wave log measures mainly the shear wave velocity in the vertical direction along the borehole, while the Stoneley mainly measures the shear wave velocity in the horizontal direction perpendicular to the borehole. Thus a combination of these measurements may allow us to further characterize the formation in terms of velocity anisotropy.

The phase velocities of the Stoneley wave are also affected by the mechanical properties of a transversely isotropic formation (White and Tongtaow 1981; Ellefsen 1990). In the case of a transversely isotropic formation with its symmetry axis parallel to the borehole, Stoneley wave phase velocity is sensitive to c_{66} at low frequency, and to c_{44} at high frequency. These sensitivities are the basis of the borehole Stoneley wave inversion in the transversely isotropic formation. However, these analyses are restricted to a borehole in line with the axis of symmetry of the transversely anisotropic formation. For a borehole normal to the axis of symmetry of a transversely anisotropic formation (creating a situation with azimuthal anisotropy), there is no analytic solution as of yet, but Ellefsen et al. (1991) have obtained numerical solutions for the phase velocity dispersion of the Stoneley wave using the Finite Element Method.

We examined a data set provided to us by Dr. Ken Tubman of ARCO which has both full waveform and shear wave logging data, in addition to some core description. The interval consists of a shale cap section (at around 3690 ft) overlying a fractured and porous permeable sand (about 3700 to 3800 ft). The inverted formation shear wave velocity (from Stoneley wave velocity assuming an isotropic model) and the dipole measured shear wave velocity are plotted in Figure 1. In this data set there is one section in the sand (3715 to 3780 ft) in which the inverted shear wave velocities disagree with the dipole shear wave velocities. This disagreement is beyond the errors in the measurements. A possible interpretation of the difference in the shear wave velocities from the two tools is formation anisotropy. As discussed earlier, in a transversely anisotropic formation with the axis of symmetry in line with the borehole, the shear wave velocity measured by the dipole tool is the vertical shear wave velocity, while that measured by the Stoneley wave is the horizontal shear wave velocity (Ellefsen et al., 1991). In the case of a layering of shale, the dipole shear wave velocity should be slower than the inverted one. This is confirmed in the shale section at around 3690 ft in the data. In the permeable sand section, the problem is much more complicated. Here we have the dipole shear wave velocity higher than the inverted shear wave velocity. The core samples indicate a high permeability (1 to 10 darcies) zone in this section. However, our calculations showed that the high permeabilities are not nearly enough to explain the abnormally low Stoneley wave velocities which resulted in the low inverted shear wave velocity. Our interpretation of this result is that the permeable formation is fractured. This fact was noted in the core description. Unfortunately no further description for the fractures was given. We are assuming that the fractures are subvertical, creating a situation where there is azimuthal anisotropy.

Under these assumptions, we can go ahead and interpret our results. In most cases, the dipole shear wave log measures the fastest velocity in the vertical direction, the exception being the case where the dipole is lined up in the slow azimuthal direction (Ellefsen et al., 1991). The Stoneley wave, on the other hand, measures a mixture of the fast and slow shear wave velocities. Under a zero frequency assumption, Rice (1987) stated that the Stoneley wave will measure the slow shear wave velocity. However, the numerical simulations of Ellefsen et al. (1991) showed that the Stoneley wave actually measures a weighted average of the fast and slow shear wave velocities, about a ratio of 2 to 1 for fast to slow, although the exact combination is not available at this time.

Using both the results of Rice (1987) and Ellefsen et al. (1991), and assuming that the dipole shear wave log measures the fast shear wave velocity, we can estimate the azimuthal shear wave velocity anisotropy in the fractured, high permeability section. Figure 2 shows the shear wave velocities estimated using the results of Rice (1987) and Ellefsen et al. (1991) and the resulting shear wave anisotropy. The degree of shear wave anisotropy seen in the permeable zone is around 5 to 15%, not unreasonable for a fractured rock.

There is one more check on the assumption of azimuthal anisotropy. In the full waveform data in the permeable zone (3700 to 3780 ft), there appears to be a "shear/ pseudo-Rayleigh" wave arrival in front of the Stoneley wave. Given the Stoneley wave velocity and the inverted shear wave velocity based on an isotropic elastic model, the formation is "slow" and there should not be a "shear/pseudo-Rayleigh" arrival. Despite this, we went ahead and estimated the phase velocity of this arrival using the semblance cross-correlation (Kimball and Marzetta, 1984; Block et al., 1991). The results are plotted in Figure 3 together with the dipole shear wave velocity and the inverted shear wave velocity from the Stoneley wave.

There are a couple of observations we can draw from Figure 3. If our hypothesis of azimuthal anisotropy is correct, then it appears that the observed arrival in the array sonic data does travel with the velocity of the fast shear wave velocity. Moreover, it gives the fastest shear wave velocity all along the fractured sandstone section. This is understandable since its frequency is around 6 kHz as opposed to the 2 kHz flexural wave generated by the dipole tool. Thus the dipole tool may tend to average the surrounding slower velocities in the formation. Furthermore, this arrival travels with a velocity greater than 1500 m/s, thus supporting the idea that this is some sort of a "refracted shear/ pseudo-Rayleigh" arrival.

A second observation is that the dipole shear wave tool does not always measure the fastest shear wave velocity. It is evident that above around 3710 ft the dipole is tracking the "slow" shear wave velocity while the "refracted shear" arrival in the array sonic is actually tracking the "fast" shear wave velocity in this fractured sandstone formation. Below 3710 ft the dipole shear wave log starts to track the "fast" arrival, although for the most part it is still a little slower than that for the array sonic, probably because of the lower frequency content. This is probably the result of tool rotation in the dipole tool. This also points out the importance of a combined integrated interpretation of both the full waveform array sonic and the dipole log. Using only one or the other could lead to an erroneous interpretation.

Crack Model for an Anisotropic Medium

Crack-induced anisotropy is of extreme importance in a large number of geophysical applications ranging from earthquake prediction to petroleum and geothermal exploration. The concept of shear-wave splitting through a cracked or fractured medium is widely accepted and is considered to be diagnostic of such a medium. Furthermore, given the observed shear-wave splitting and velocity anisotropy, such as we have seen in the data shown in the previous section, one can attempt to obtain crack or fracture parameters such as crack density by the use of a crack model. A commonly used crack-induced seismic-anisotropy model is that of Hudson (1980, 1981), which is based on a scattering formulation for very small-aspect-ratio (thickness over length) cracks.

It is well known that at higher crack densities, the second-order term in Hudson's expansion begins to dominate over the first-order term, causing the effective moduli to increase instead of decrease with increasing crack density. This effect can occur at relatively small crack densities (about 0.19 for the compressive moduli with empty cracks). The whole idea of having a higher order expansion is to try to extend the first-order theory to higher crack densities. However, because of the nature of the expansion, this is not possible under the present form. Furthermore, the multi-valued nature of the Hudson second order expansion makes the interpretation in terms of crack density from the observed seismic anisotropy difficult and ambiguous. By examining this nature and by comparison with a well known exact solution for a spherical cavity, we developed a new expansion based on the Padé approximation. The Padé approximation is frequently used to evaluate functions which are divergent if expanded in a power series representation (Bender and Orszag, 1978; Press and Teukolsky, 1992). It is based on a ratio of two power series. By suitably matching the coefficients, we can obtain an expansion that is identical to the Hudson expansion up to the second-order in crack density. Moreover, we can demonstrate that this expansion is monotonically decreasing with crack density for all crack densities. We suggest that this new form should be more accurate to a higher crack density. An example for empty cracks in a Poisson solid is shown in Figure 4.

Numerical Simulation of Flow through Rough Surfaces

In many applications where the pressure gradient driving fluid through a porous permeable medium is time invariant, steady-state (time-independent) flow is assumed and the flow can be modeled for any distribution of heterogeneous porous media using a finite-difference technique (Zhao and Toksöz, 1991). When the pressure gradient changes moderately with time, such as the pressure transient tests in a borehole (Melville et al., 1991) and in some laboratory measurements (Brace et al., 1968; Kamath et al., 1990; Bernabé, 1991), fluid flow can be modeled as a diffusion process in which the fluid transport properties such as permeability are the same as under steady flow conditions. However, in applications related to wave propagation, such as vertical seismic profiling and acoustic logging, where the pressure gradient changes rapidly with time, the transport properties become frequency dependent.

To characterize the frequency-dependent fluid transport property, Johnson et al. (1987) developed the theory of dynamic permeability. Applying the concept of dynamic permeability to the problem of acoustic logging in permeable porous formations, Tang et al. (1991) showed that the dynamic permeability captures the frequency-dependent behavior of Biot's (1956a,b) slow wave and correctly predicts the effects of formation permeability on borehole Stoneley waves. The theory of dynamic permeability is formulated assuming the homogeneity of the porous medium. The natural geological medium, however, contains heterogeneities of various scales. It would be interesting to apply the dynamic permeability to the heterogeneous porous media to study the overall behavior of fluid flow through the media. We have modeled the dynamic fluid flow in the heterogeneous porous media using the theory of dynamic permeability. A finite-difference method has been developed to model the effects of heterogeneities.

A similar problem that has attracted much research interest is fluid flow through a rough-walled fracture or joint. Brown (1987, 1989) and Zimmerman et al. (1991) have modeled the steady-state fluid flow through the fracture and showed that the roughness of the fracture surfaces significantly affects the fluid flow when the surfaces are in contact. In the characterization of borehole fractures using acoustic logging (Paillet et al., 1989; Hornby et al., 1989), the response of the fracture to the dynamic pressure set up by the logging waves is important for characterizing the fracture permeability. In this situation, fluid flow in fractures is dynamic in nature. Tang and Cheng (1989) have studied the dynamic flow through a plane fracture bounded by two parallel walls. Natural fracture surfaces, however, exhibit roughness (Brown, 1987). It is important to understand the effects of surface roughness on the dynamic fluid flow in order to correctly model the dynamic response of natural fractures to borehole acoustic waves. Tang et al. (1991) have shown that the theory of dynamic permeability, when applied to the parallel-wall fracture, is equivalent to the theory of fracture dynamic conductivity. Therefore, if we assume that the dynamic permeability for a parallel-wall fracture holds locally in a fracture, then we can use the finite-difference code developed for heterogeneous porous media to model the dynamic flow in a rough-walled fracture.

An iterative Alternating Direction Implicit finite-difference technique is applied to calculate the flow field in the frequency domain. We compare the flow through a 2-D heterogeneous porous medium and that through an equivalent homogeneous medium and find that the two media do not behave equivalently as a function of frequency. At very low-frequencies, the heterogeneous medium is less conductive than the homogeneous medium. However, in the transition region from quasi-static to dynamic regimes, the former medium becomes more conductive than the latter medium, with the ratio of the former flow over the latter flow reaching a maximum in this region. The larger the scale, or the higher the degree of the heterogeneity, the higher this maximum is. This finding is important for studying the interaction of the borehole Stoneley wave with a heterogeneous porous formation. In the logging situation, the formation may contain various heterogeneities and the heterogeneous flow behavior can cause discrepancies between the field observations and the theoretical predictions from Biot's theory for a homogeneous medium.

The finite-difference technique is also applied to simulate frequency-dependent flow through a single fracture with rough surfaces. It is shown that the flow exhibits strong frequency-dependence even for small fractures with contacting surfaces. For dynamic as well as steady flow cases, the surface roughness reduces the amount of fluid flow through the fracture in the static and dynamic regimes as compared to the parallel wall model. When the separation between the two fracture surfaces is about 10 times the standard deviation of the roughness, the behavior of the fracture approaches that of a parallel plane fracture. A complete description of the results is contained in Zhao et al. (1992) and is included here as Appendix B.

Seismic Imaging of Hydrofrac using Microearthquake Travel Time Data:

In cooperation with Dr. Michael Fehler and Dr. Scott Phillips of Los Alamos National Laboratory, a detailed study of the joint hypocenter-velocity inversion was carried out using microearthquake arrival time data from the Los Alamos Hot Dry Rock geothermal site. The goal was to determine if this type of inversion could improve the earthquake locations and if the three-dimensional P-wave and S-wave velocity structures of the fractured reservoir could be determined. The strengths and limitations of the method, as applied to this data set, were investigated. The results are presented in Block et al. (1992, enclosed here as Appendix C) and summarized below.

The joint hypocenter-velocity inversions yield S wave velocity structures which generally correlate well with the earthquake locations. Studies of synthetic data show that the locations and general shapes of the V_S anomalies are reliable in regions where the ray coverage is adequate. The magnitudes of the velocities cannot be precisely determined. The percent velocity perturbations increase as the velocity regularization weighting of the inversion decreases. Studies of inversions performed using different regularization weightings suggest that the S-wave velocities decrease by at least 13% in the most intensively fractured regions of the reservoir.

The joint inversions yield very smooth P-wave velocity structures. The minimum P-wave velocities occur in an aseismic region, decreasing as much as 22 – 43% compared to the velocity of the unfractured rock. Presence of these very low P-wave velocities in an aseismic region is not consistent with the hypothesis that the fractured reservoir is defined by the earthquake locations. Also, if no constraints are applied to the V_P/V_S ratios, then the V_P/V_S structures computed from the final V_P and V_S models display a broad, pronounced minimum at the location of the lowest V_P values. The minimum V_P/V_S values range from 1.06 to 1.38, depending on the amount of velocity regularization applied. These values are not reasonable either for the mostly unfractured rock outside the reservoir or for the rock containing fluid-filled fractures within the reservoir. Synthetic data simulations demonstrate that the P-wave velocity models and the V_P/V_S structures determined by the joint inversion are not reliable for the given station geometry. Since the travel time perturbations caused by the fluid-filled fractures are much smaller for P waves than for S waves, the P-wave velocities are less constrained by the data than the S-wave velocities. If the data variance from other sources — such as arrival time picking errors, velocity variations outside the inversion grid, and velocity anisotropy — is as large as the perturbations due to the fractured reservoir, the shape of the reservoir is not resolved in the final V_p model. Rather, the P-wave velocity structure is strongly influenced by the velocity regularization, which biases the V_p model toward a smoother shape. This bias results in erroneous V_p/V_s ratios.

If no constraints are applied to the V_p/V_s ratios, then the hypocenters are rotated into a more vertical and more North-South orientation during the joint inversion of the Los Alamos data. As synthetic data tests show, the poor V_p/V_s ratios cause systematic error in the earthquake locations. Hence, the earthquake rotation observed in the inversions of the field data is an artifact of the error in the P-wave velocity structure. The trade-offs between the V_p/V_s ratios and the earthquake locations are strong for this problem because the azimuthal ray coverage with the four seismometers is poor.

Inversions performed with a lower bound of 1.60 applied to the V_p/V_s ratios yield models which satisfy the data as well as the models from the inversions performed without the bound, and they yield more geologically reasonable V_p/V_s structures. The residuals decrease 11 – 15% during the inversions. The P-wave velocity structure is much more strongly affected by the addition of the V_p/V_s bound than the S-wave velocity structure. This observation is consistent with the hypothesis given above that the P-wave velocities are not constrained by the data as well as the S-wave velocities. For these inversions, the final earthquake locations are *not* systematically rotated with respect to the initial locations. The average absolute change in the earthquake locations during these inversions is 20 – 27 m. Unfortunately, given the non-uniqueness of the inversion results, it is impossible to claim simply from the reduction in the residuals that the earthquake locations have been improved by the joint inversion. Future studies may indicate whether the new locations better define the major fracture planes of the reservoir.

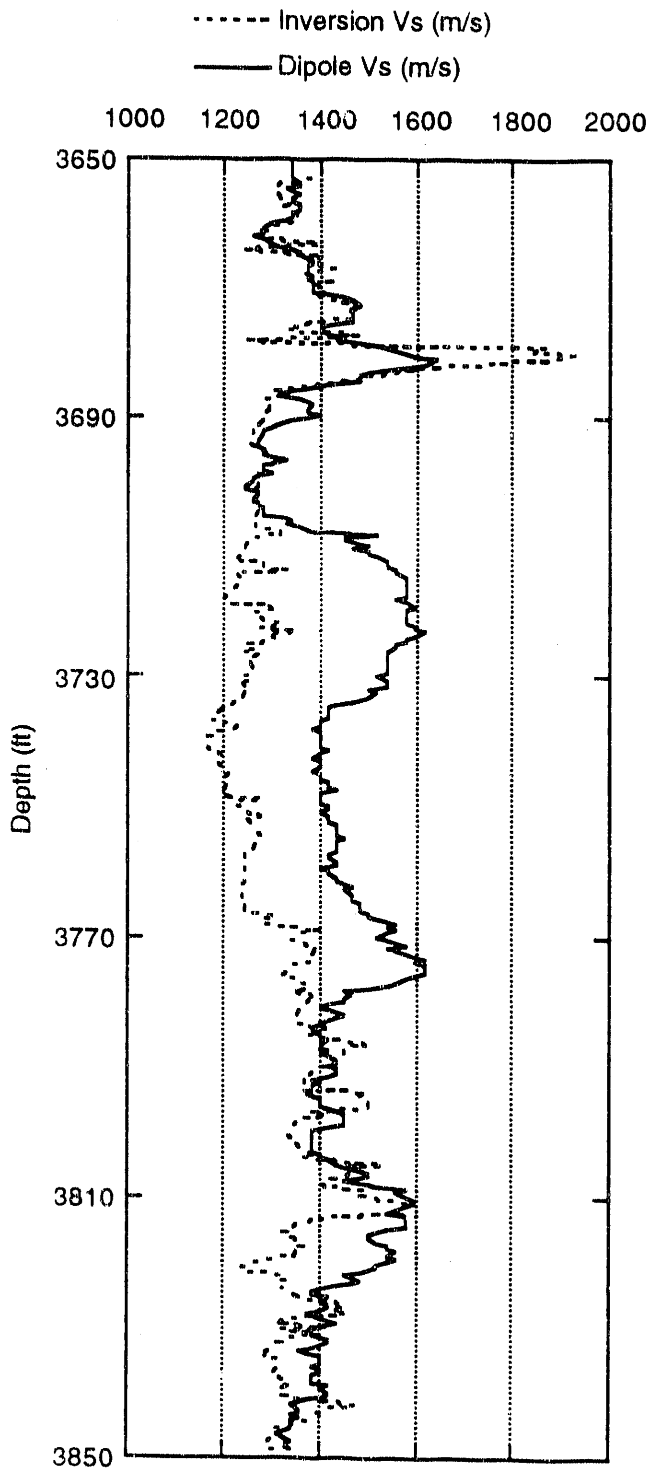

Figure 1: Inversion results for the ARCO data. The formation V_S from inverted Stoneley wave velocity is shown with the shear wave log V_S.

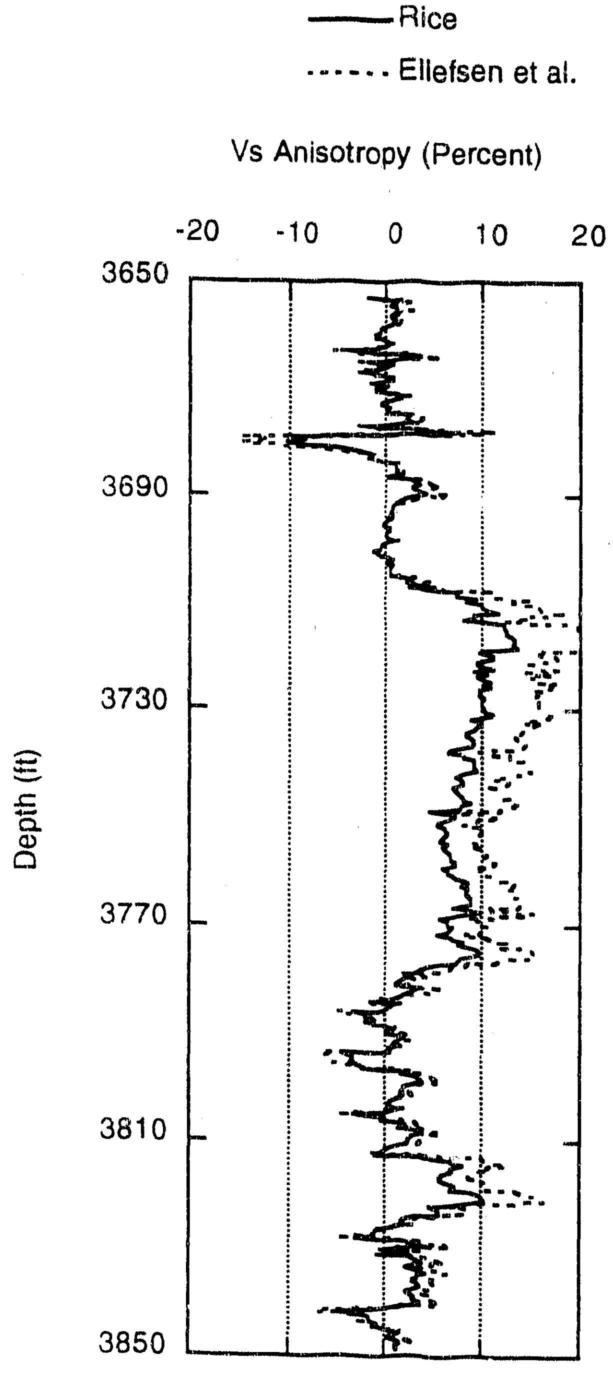

Figure 2: Shear wave anisotropy determined using the Rice (1987) and the Ellefsen et al. (1991) assumptions.

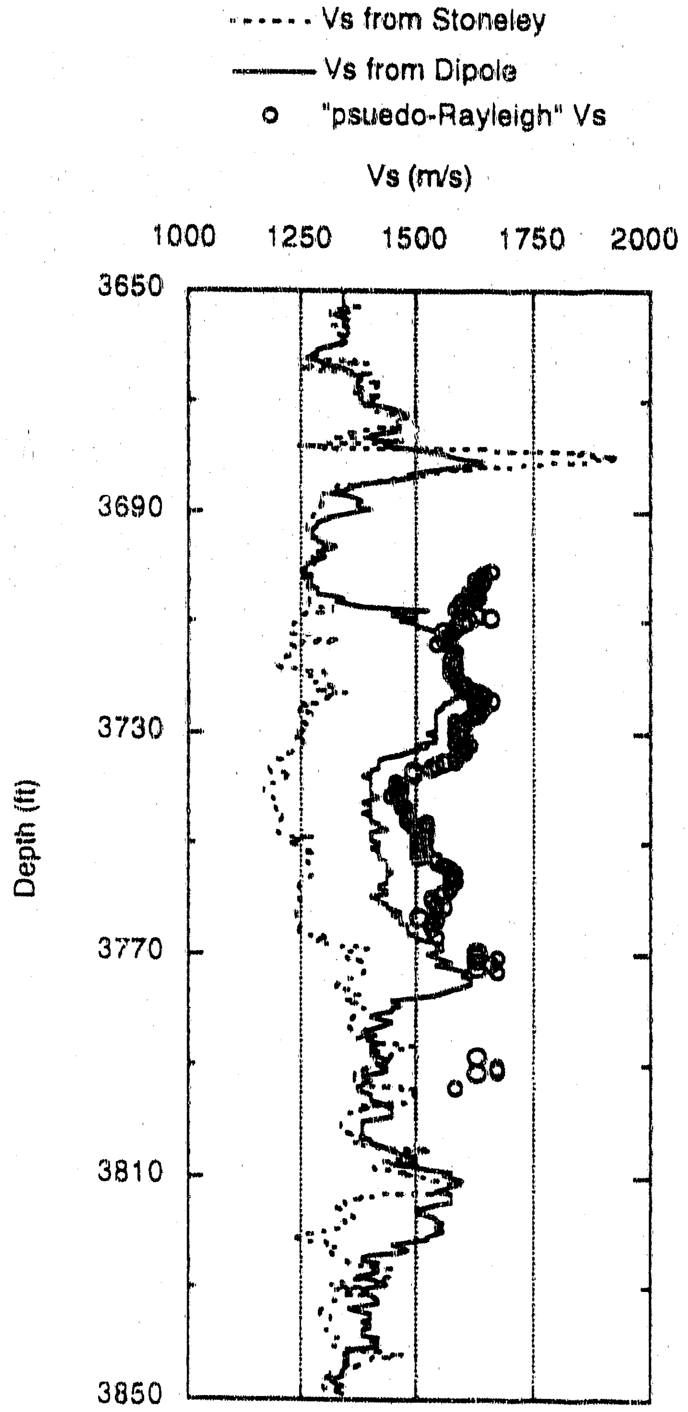

Figure 3: Shear wave velocity determined from inverted Stoneley wave velocity as compared with V_S from the dipole tool and the velocity from the "refracted shear/pseudo-Rayleigh" arrival in the array sonic data.

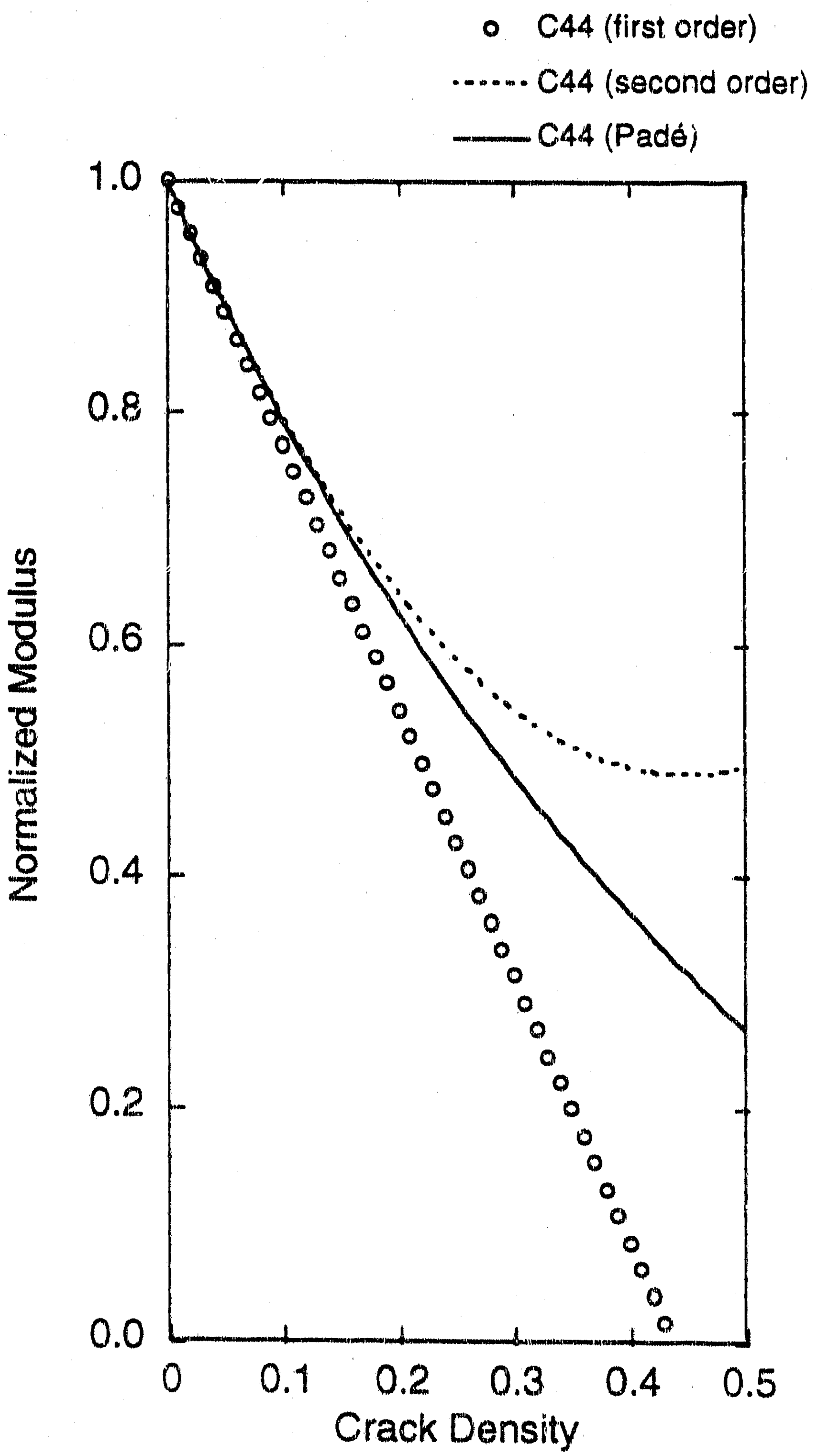

Figure 4: Comparison of first order, second order, and Padé expansion for normalized c_{44} for dry cracks.

REFERENCES

Bender, C.M., and S.A. Orszag, *Advanced Mathematical Methods for Scientists and Engineers*, McGraw-Hill, New York, 1978.

Bernabé, Y., 1991, On the measurement of permeability in anisotropic rocks, *in Fault Mechanism and Transport Properties of Rocks: A Festchrift in Honor of W.F. Brace edited by B.J. Evans and T.F. Wong, in press,* Academic Press, London.

Bhashvanija, K., *A finite difference model of an acoustic logging tool: The borehole in a horizontal layered geologic medium,* Ph.D. Thesis, Colorado School of Mines, Golden, CO., 1983.

Biot, M.A., Theory of propagation of elastic waves in a fluid-saturated porous solid, I: Low frequency range, *J. Acoust. Soc. Am., 28,* 168–178, 1956a.

Biot, M.A., Theory of propagation of elastic waves in a fluid-saturated porous solid, II: Higher frequency range, *J. Acoust. Soc. Am., 28,* 179–191, 1956b.

Brace, W.F., J.B. Walsh, and W.T. Frangos, Permeability of granite under high pressure, *J. Geophys. Res., 73,* 2225–2236, 1968.

Brown, S.R., Flow through rock joints: the effect of surface roughness, *J. Geophys. Res., 92,* 1337–1347, 1987.

Brown, S.R., Transport of fluid and electric current through a single fracture, *J. Geophys. Res., 94,* 9429–9438, 1989.

Block, L.V., C.H. Cheng, and G.L. Duckworth, Velocity analysis of multi-receiver full waveform acoustic logging data in open and cased holes, *The Log Analyst, 32,* 188–200, 1991.

Block, L.V., C.H. Cheng, M.C. Fehler, and W.S. Phillips, Seismic imaging using microearthquakes induced by hydraulic fracturing, *Geophysics,* submitted, 1992.

Ellefsen, K.L., *Elastic wave propagation along a borehole in an anisotropic medium,* Ph.D. Thesis, Massachusetts Institute of Technology, Cambridge, Mass., 1990.

Ellefsen, K.L., C.H. Cheng, and M.N. Toksöz, Effects of anisotropy upon the normal modes in a borehole, *J. Acoust. Soc. Am., 89,* 2597–2616, 1991.

Hardin, E.L., C.H. Cheng, F.L. Paillet, and J.D. Mendelson, Fracture characterization by means of attenuation and generation of tube waves in fractured crystalline rock at Mirror Lake, New Hampshire, *J. Geophys. Res., 92,* 7989–8006, 1987.

Hornby, B.E., D.L. Johnson, K.H. Winkler, and R.A. Plumb, Fracture evaluation using reflected Stoneley-wave arrivals, *Geophysics, 54,* 1274–1288, 1989

Hudson, J.A., Overall properties of a cracked solid, *Math. Proc. Camb. Phil. Soc., 88,* 371–384, 1980.

Hudson, J.A., Wave speeds and attenuation of elastic waves in materials containing cracks, *Geophys. J. Roy. Astr. Soc., 64,* 133–150, 1981.

Johnson, D.L., J. Koplik, and R. Dashen, Theory of dynamic permeability and tortuosity in fluid-saturated porous media, *J. Fluid Mech., 176,* 379–400, 1987.

Kamath, J., R.E. Boyer, and F.M. Nakagawa, Characterization of core scale heterogeneities using laboratory pressure transients, *Society of Petroleum Engineers,* 475–488, 1990.

Kimball, C.V., and T.L. Marzetta, Semblance processing of borehole acoustic array data, *Geophysics, 49,* 274–281, 1984.

Melville, J.G., F.J. Molz, O. Göven, and M.A. Widdowson, Multilevel slug tests with comparisons to tracer data, *Ground Water, 29,* 897–907, 1991.

Paillet, F.L., Acoustic propagation in the vicinity of fractures which intersect a fluid-filled borehole, *Trans. SPWLA 21st Ann. Symp.*, Paper DD, 1980.

Paillet, F.L., and J.E. White, Acoustic modes of propagation in the borehole and their relationship to rock properties, *Geophysics, 47,* 1215–1228, 1982.

Paillet, F.L., C.H. Cheng, and X.M. Tang, Theoretical models relating acoustic tube-wave attenuation to fracture permeability — reconciling model results with field data, *Trans. SPWLA 30th Ann. Symp.*, Paper FF, 1989.

Press, W.H., and S.A. Teukolsky, Padé Approximants, *Comp. in Phys., 6,* 82–83, 1992.

Pride, S.R., F.D. Morgan, and A.F. Gangi, Modeling the drag forces of porous media acoustics, *Physical Review B,* submitted, 1992.

Rice, J.A., A method of logging shear wave anisotropy, *57th SEG Ann. Mtg. Expanded Abstracts,* 27–28, 1987.

Rosenbaum, J.H., Synthetic microseismograms: logging in porous formations, *Geophysics, 39,* 14–32, 1974.

Schmitt, D.P., M. Bouchon, and G. Bonnet, Full-wave synthetic acoustic logs in radially semi-infinite saturated porous media, *Geophysics, 53,* 807–823, 1988.

Stephen, R.A., F. Pardo-Casas, and C.H. Cheng, Finite difference synthetic acoustic logs, *Geophysics, 50,* 1588–1609, 1985.

Stevens, J.L., and S.M. Day, Shear velocity logging in slow formations using the Stoneley wave, *Geophysics, 51,* 137–147, 1986.

Tang, X.M., *Acoustic logging in fractured and porous formations,* Sc.D. Thesis, Massachusetts Institute of Technology, Cambridge, MA., 1990.

Tang, X.M., and C.H. Cheng, A dynamic model for fluid flow in open borehole fractures, *J. Geophys., Res., 94,* 7567–7576, 1989.

Tang, X.M., C.H. Cheng, and M.N. Toksöz, Dynamic permeability and borehole Stoneley waves: A simplified Biot-Rosenbaum model, *J. Acoust. Soc. Am., 90,* 1632–1646, 1991.

Tang, X.M., and C.H. Cheng, Borehole Stoneley wave propagation across heterogeneous and permeable structures, *Geophys. Prop.,* submitted, 1992.

White, J.E., and C. Tongtaow, Cylindrical waves in transversely isotropic media, *J. Acoust. Soc. Am., 70,* 1147–1155, 1981.

Zemanek, J., F.A. Angona, D.M. Williams, and R.L. Caldwell, Continuous acoustic shear wave logging, *Trans. SPWLA 25th Ann. Logging Symp., New Orleans,* Paper U, 1984.

Zhao, X.M., and M.N. Toksöz, Permeability anisotropy in heterogeneous porous media, *61st SEG Ann. Mtg. Expanded Abstracts,* 387–390, 1991.

Zhao, X., C.H. Cheng, X.M. Tang, and M.N. Toksöz, Dynamic fluid flow in heterogeneous porous media and through a single fracture with rough surfaces, *M.I.T. Borehole Acoustics and Logging Consortium Annual Report,* 157–177, 1992.

Zimmerman, R.W., S. Kumar, and G.S. Bodvarsson,, Lubrication theory analysis of the permeability of rough-walled fractures, *Int. J. Rock. Mech. Min. Sci. & Geomech. Abstr., 28,* 325–331 1991.

PUBLICATIONS SUPPORTED BY EXISTING GRANT:

Tang, X.M., M.N. Toksöz, P.A. Tarif, and R.H. Wilkens, A method of measuring acoustic wave attenuation in the laboratory, *J. Acoust. Soc. Am., 83,* 453–462, 1988.

Tang, X.M., and C.H. Cheng, Wave propagation in a fluid-filled fracture — an experimental study, *Geophys. Res. L., 15,* 1463–1466, 1988.

Tang, X.M., and C.H. Cheng, A dynamic model for fluid flow in open borehole fractures, *J. Geophys. Res., 94,* 7567–7576, 1989.

Paillet, F., C.H. Cheng, and X.M. Tang, Theoretical models relating acoustic tube-wave attenuation to fracture permeability — reconciling model results with field data, *Trans. SPWLA 30th Ann. Logging Symp.,* Paper FF, 1989.

Tang, X.M., M.N. Toksöz, and C.H. Cheng, Elastic wave diffraction of a piston source and its effect on attenuation measurement, *J. Acoust. Soc. Am., 87,* 1894–1902, 1990.

Tang, X.M., Acoustic logging in fractured and porous formations, Sc.D. Thesis, M.I.T., Cambridge, MA., 1990.

Gibson, R.L., and M.N. Toksöz, Permeability estimation from velocity anisotropy in fractured rock, *J. Geophys. Res., 95,* 15643–15655, 1990.

Tang, X.M., C.H. Cheng, and M.N. Toksöz, Stoneley wave propagation in a fluid-filled borehole with a vertical fracture, *Geophysics, 56,* 447–460, 1990.

Tang, X.M., C.H. Cheng, and M.N. Toksöz, Dynamic permeability and borehole Stoneley waves: a simplified Biot-Rosenbaum model, *J. Acoust. Soc. Am., 90,* 1632–1646, 1991.

Tang, X.M., C.H. Cheng, and F.L. Paillet, Modeling borehole Stoneley wave propagation across permeable in-situ fractures, *Trans. SPWLA 32th Ann. Logging Symp.,* Paper GG, 1991.

Block, L.V., Joint hypocenter-velocity inversion of local earthquake arrival time data in geothermal regions, Sc.D. Thesis, M.I.T., Cambridge, MA., 1991.

Zhao, X., and M.N. Toksöz, Characterizing surface roughness from pressure-joint closure measurements using inversion procedure, *Geophys. Res. L., 19,* 123–126, 1992.

Toksöz, M.N., C.H. Cheng, and R.D. Cicerone, Fracture detection and characterization from hydrophone VSP data, in *Fault Mechanics and Transport Properties of Rock,* B. Evans (ed.), in press, Academic Press, 1992.

Tang, X.M., and C.H. Cheng, Effects of a logging tool on the Stoneley waves in elastic and porous boreholes, *The Log Analyst, in press,* 1992.

Cheng, C.H., Crack models for a transversely isotropic medium, *J. Geophys. Res.,* in press, 1992.

Block, L.V., C.H. Cheng, M.C. Fehler, and W.S. Phillips, Seismic imaging using microearthquakes induced by hydraulic fracturing, *Geophysics,* submitted, 1992.

Tang, X.M., and C.H. Cheng, Borehole Stoneley wave propagation across hetergeneous and permeable structures, *Geophys. Prop.,* submitted, 1992.

Zhao, X., and M.N. Toksöz, Permeability anisotropy in heterogeneous porous media, *J. Geophys. Res.,* submitted, 1992.

PRESENTATIONS SUPPORTED BY EXISTING GRANT:

Tang, X.M., M.N. Toksöz, P.A. Tarif, and R.H. Wilkens, A method of measuring acoustic wave attenuation in the laboratory, *Soc. Expl. Geophys. 57th Ann. Internat. Mtg.*, New Orleans, October 11–15, 1987.

Cheng, C.H., Fracture characterization using hydrophone and 3-component VSPs at Fenton Hill, *Am. Geophys. Union Fall Mtg.*, San Francisco, December 7–11, 1987.

Cheng, C.H., Characterization of fluid flow in fractured rocks using borehole seismic methods, *Internat. Conf. on Fluid Flow in Fractured Rocks*, Atlanta, May 15–18, 1988.

Tang, X.M., M.N. Toksöz, and C.H. Cheng, Elastic wave diffraction of a piston source and its effect on attenuation measurements, *Soc. Expl. Geophys. 58th Ann. Internat. Mtg.*, Anaheim, October 30–November 3, 1988.

Tang, X.M., and C.H. Cheng, A dynamic model for fluid flow in open borehole fractures, *Am. Geophys. Union Fall Mtg.*, San Francisco, December 5–9, 1988.

Tang, X.M., C.H. Cheng, and M.N. Toksöz, Stoneley wave propagation in a fluid-filled borehole with a vertical fracture, *Soc. Expl. Geophys. 59th Ann. Internat. Mtg.*, Dallas, October 29–November 2, 1989.

Gibson, R.L., and M.N. Toksöz, Permeability estimation from velocity anisotropy in fractured rock, *Soc. Expl. Geophys. 59th Ann. Internat. Mtg.*, Dallas, October 29–November 2, 1989.

Block, L.V., C.H. Cheng, and M.C. Fehler, The velocity structure of the Los Alamos Hot Dry Rock reservoir: Inversion of microearthquake arrival time data, *Am. Geophys. Union Fall Mtg.*, San Francisco, December 4–8, 1989.

Ellefsen, K.J., C.H. Cheng, and M.N. Toksöz, Seismic wave propagation in a borehole through an anisotropic formation, *Am. Geophys. Union Fall Mtg.*, San Francisco, December 4–8, 1989.

Block, L.V., C.H. Cheng, and M.N. Toksöz, The velocity structure of the Larderello geothermal field: inversion of local earthquake arrival time data, *Am. Geophys. Union Spring Mtg.*, Baltimore, May 29–June 1, 1990.

Tang, X.M., C.H. Cheng, and M.N. Toksöz, Dynamic permeability and borehole Stoneley waves: a simplified Biot-Rosenbaum model, *SEG Research Workshop on Permeability, Fluid Pressure and Pressure Seals in the Crust*, Denver, August 5–8, 1990.

Gibson, R.L., and M.N. Toksöz, Permeability estimation from velocity anisotropy in fractured rock, *SEG Research Workshop on Permeability, Fluid Pressure and Pressure Seals in the Crust*, Denver, August 5–8, 1990.

Tang, X.M., C.H. Cheng, and M.N. Toksöz, Dynamic permeability and borehole Stoneley waves: a simplified Biot-Rosenbaum model, *Soc. Expl. Geophys. 60th Ann. Internat. Mtg.*, San Francisco, September 23–27, 1990.

Block, L.V., C.H. Cheng, M.C. Fehler, and W.S. Phillips, Inversion of microearthquake arrival time data at the Los Alamos Hot Dry Rock Reservoir, *Soc. Expl. Geophys. 60th Ann. Internat. Mtg.*, San Francisco, September 23–27, 1990.

Block, L.V., M.N. Toksöz, and F. Batini, Crustal velocity structure of the Larderello geothermal field determined from local earthquake arrival time data, *Eur. Assoc. of Expl. Geophys. 53rd Mtg.*, Florence, Italy, May 26–30, 1991.

Tang, X.M., and C.H. Cheng, Borehole Stoneley wave propagation across heterogeneous and permeable structures, *Eur. Assoc. of Expl. Geophys. 53rd Mtg.*, Florence, Italy, May 26–30, 1991.

Tang, X.M., C.H. Cheng, and F.L. Paillet, Modeling borehole Stoneley wave propagation across permeable in-situ fractures, *SEG Research Workshop on Lithology*, St. Louis, July 28–August 1, 1991.

Zhao, X., and M.N. Toksöz, Modeling fluid flow in heterogeneous and anisotropic porous media, *Soc. Expl. Geophys. 61th Ann. Internat. Mtg.*, Houston, November 10–14, 1991.

Tang, X.M., and C.H. Cheng, Borehole Stoneley wave propagation across permeable fractures, *Soc. Expl. Geophys. 61th Ann. Internat. Mtg.*, Houston, November 10–14, 1991.

Cheng, C.H., Comments on crack models for a transversely anisotropic medium, *Am. Geophys. Union Fall Mtg.*, San Francisco, December 9–13, 1991.

Cicerone, R.D., and M.N.Toksöz, Fracture characterization from vertical seismic profiling data, *Am. Geophys. Union Fall Mtg.*, San Francisco, December 9–13, 1991.

END

DATE FILMED

10 / 14 / 92